

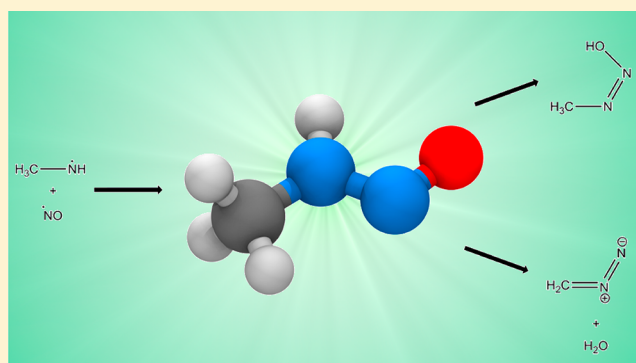
Formation of Nitrosamines and Alkyldiazohydroxides in the Gas Phase: The $\text{CH}_3\text{NH} + \text{NO}$ Reaction Revisited

Gabriel da Silva*

Department of Chemical and Biomolecular Engineering, The University of Melbourne, Victoria 3010, Australia

Supporting Information

ABSTRACT: Aminyl free radicals of the form $\text{RN}^\bullet\text{H}$ are formed in the photochemical oxidation of primary amines, and their reaction with $^\bullet\text{NO}$ is an important tropospheric sink. Reaction of the parent methylamidogen radical ($\text{CH}_3\text{N}^\bullet\text{H}$) with $^\bullet\text{NO}$ in the gas phase has been studied using quantum chemical techniques and RRKM theory/master equation based kinetic modeling. Calculations with the G3X-K composite theoretical method indicate that reaction proceeds via exothermic formation of a primary nitrosamine intermediate, CH_3NHNO , which can isomerize to an alkyldiazohydroxide, CH_3NNOH , and further eliminate water to form diazomethane, CH_2NN . Master equation simulations conducted at tropospheric conditions identify that the collisionally stabilized CH_3NHNO and CH_3NNOH isomers are the major reaction products, with smaller yields of $\text{CH}_2\text{NN} + \text{H}_2\text{O}$. A previously proposed mechanism in which the primary nitrosamine is destroyed via isomerization to CH_2NHNOH , followed by reaction with O_2 to produce $\text{CH}_2\text{NH} + \text{HO}_2^\bullet + ^\bullet\text{NO}$, is disproved. In the atmosphere, CH_2NN may be formed with sufficient vibrational energy to directly dissociate to singlet methylene ($^1\text{CH}_2$) and N_2 , whereas under combustion conditions this is expected to be the dominant pathway. This study suggests that stabilized primary nitrosamines can indeed form in the photochemical oxidation of amines, along with alkyldiazohydroxides and diazoalkanes. Both classes of compound are potent alkylating agents that may need to be considered in future atmospheric studies.



INTRODUCTION

There is at present a growing concern about the role of amines in Earth's atmosphere. Amines are released to the atmosphere through animal husbandry, biomass burning, and a variety of industrial activities, and simple primary, secondary, and tertiary alkylamines are often encountered in the troposphere at low ppb levels.^{1–3} Amines appear to play an important role in particle nucleation³ and, unlike (oxygenated) hydrocarbons, the atmospheric oxidation of amines could lead to the production of nitrogenated compounds that are highly toxic^{4,5} or potent greenhouse gases.¹ It is thus imperative that we have a complete understanding of the lifetime and fate of amines in the atmosphere.

Methylamine (CH_3NH_2) is the simplest alkylamine, and is a useful prototype for understanding the atmospheric chemistry of amines, as well as being an important trace atmospheric component in its own right. Methylamine reacts relatively rapidly with $^\bullet\text{OH}$, with $k \approx 10^{-11} \text{ cm}^3 \text{ molecule}^{-1} \text{ s}^{-1}$,^{6,7} and will be oxidized within the troposphere within around a day. The primary product of the $\text{CH}_3\text{NH}_2 + ^\bullet\text{OH}$ reaction is the aminomethyl radical, $^\bullet\text{CH}_2\text{NH}_2$.⁸

Alpha-amino substituted alkyl radicals, it has recently been revealed, react with O_2 to yield imines and the HO_2^\bullet radical.^{9–11} In the case of methylamine the principal first-

generation oxidation product will therefore be methanimine, $\text{CH}_2=\text{NH}$. A minor product in the methylamine reaction with $^\bullet\text{OH}$ appears to be the methylamidogen radical, $\text{CH}_3\text{N}^\bullet\text{H}$,⁸ estimated to account for 20% of the reaction products at room temperature. Both the $^\bullet\text{CH}_2\text{NH}_2$ and $\text{CH}_3\text{N}^\bullet\text{H}$ radicals have also been identified as products of the related methylamine + Cl^\bullet abstraction reaction.¹² The $\text{CH}_3\text{N}^\bullet\text{H}$ radical is interesting, as its further reactions allow for N–X bond formation, and can potentially lead to a diverse range of products. Moreover, because N-centered radicals typically react slowly with O_2 , this species will be removed from the atmosphere primarily through bimolecular reactions with other trace compounds, such as $^\bullet\text{NO}$ and NO_2^\bullet . The reactions of alkylamidogen (alkylaminyl) radicals with $^\bullet\text{NO}$ are of potential interest as atmospheric sources of highly carcinogenic¹³ nitrosamines. Dimethylnitrosamine (DMNA), for instance, has been detected in clouds and fogs within urban plumes at concerning levels.^{14,15} Atmospheric modeling supports gas-phase chemistry as the source of aqueous nitrosamines,¹⁵ as opposed to the direct aqueous-

Received: April 11, 2013

Revised: June 17, 2013

Accepted: June 20, 2013

Published: June 20, 2013

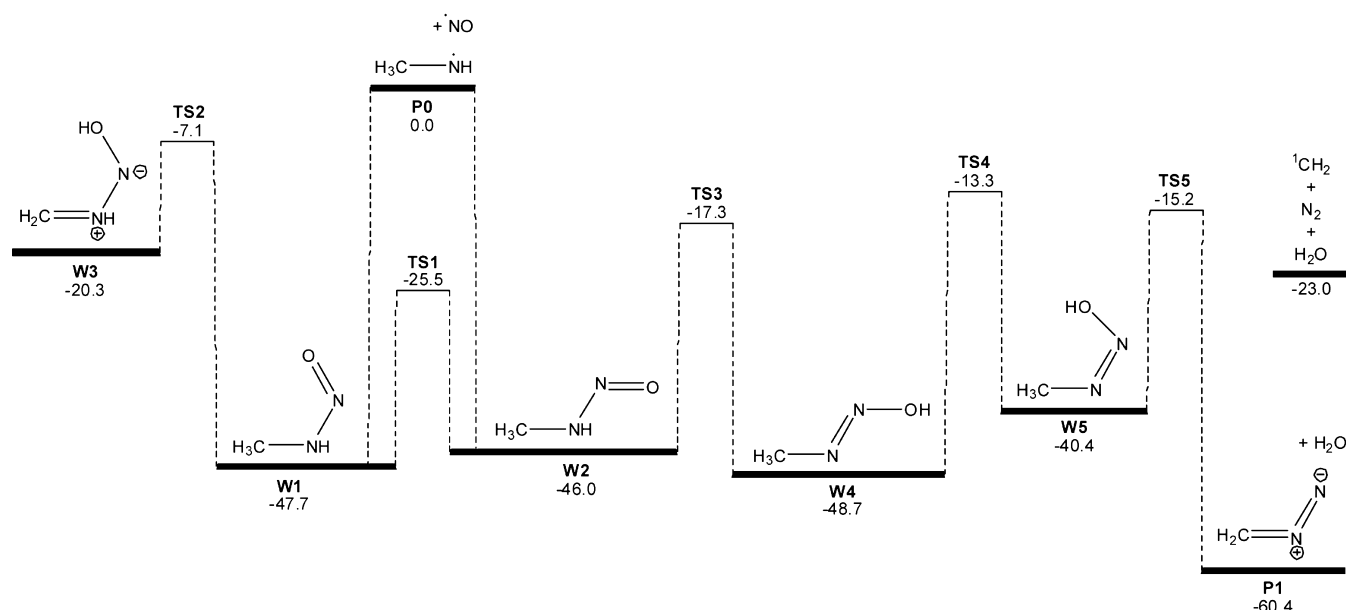


Figure 1. Energy diagram for the $\text{CH}_3\text{NH}^\bullet + \bullet\text{NO}$ reaction, at the G3X-K level of theory (relative 0 K enthalpies in kcal mol^{-1}). Energy level for the further dissociation products of P1 ($^1\text{CH}_2 + \text{N}_2 + \text{H}_2\text{O}$) also indicated.

phase nitrosation of amines which proceeds via reactions of acidified nitrite.¹⁶ Note, however, that in marine aerosols elevated levels of the halide ions Br^- and I^- may be able to act as potent nitrosation catalysts,^{17,18} potentially increasing the importance of aqueous-phase chemistry in these areas. Interestingly this mechanism appears to be previously unconsidered in the atmospheric environment.

The $\text{CH}_3\text{N}^\bullet\text{H} + \bullet\text{NO}$ reaction has been recently investigated using theoretical methods,¹⁹ providing important information about the mechanism of this process. It was shown that this radical–radical recombination reaction was considerably exothermic (almost 50 kcal mol^{-1}), leading to a chemically activated $[\text{CH}_3\text{NHNO}]^*$ adduct in the gas-phase. An isomerization reaction for CH_3NHNO was identified proceeding below the reactant energy to yield CH_2NHNOH at around 20 kcal mol^{-1} exothermic overall. It was proposed that the $\text{CH}_3\text{N}^\bullet\text{H} + \bullet\text{NO}$ reaction would ultimately lead to the products $\text{CH}_2\text{NH} + \text{HO}_2^\bullet + \text{N}_2$ via reaction of the CH_2NHNOH intermediate with O_2 (with a barrier of around 10 kcal mol^{-1}), thus destroying the primary nitrosamine intermediate. More recently this mechanism was also extended to the related $\text{CH}_3\text{CH}_2\text{N}^\bullet\text{H}$ radical.²⁰ However, collisional deactivation of the relatively fragile CH_2NHNOH well is unlikely in any significant yield, and so is its rapid spin-forbidden reaction with O_2 , and this has prompted us to re-examine this reaction. To this end, the $\text{CH}_3\text{N}^\bullet\text{H} + \bullet\text{NO}$ reaction is studied here using ab initio calculations and master equation kinetic modeling, in an attempt to resolve the mechanism of this reaction and identify the products formed under tropospheric conditions.

MATERIALS AND METHODS

The $\text{CH}_3\text{N}^\bullet\text{H} + \bullet\text{NO}$ reaction has been studied using G3X-K theory,²¹ a composite theoretical method designed specifically for thermochemical kinetics. This method uses M06-2X/6-31G(2df,p) optimized structures, vibrational frequencies, and scaled zero-point energies, in conjunction with a series of wave function theory single-point energy calculations using Hartree–Fock theory, perturbation theory (MP2, MP3, MP4), and

coupled cluster theory (CCSD(T)), combined with empirical scaling corrections so as to approximate the CCSD(T) energy with a large basis set. The G3X-K method is expected to be accurate to around $0.6 \text{ kcal mol}^{-1}$, on average, for barrier heights and reaction energies.²¹ All reported calculations were performed using Gaussian 09.²² Optimized structures and vibrational frequencies for wells and minima required for the master equation model are listed in the Supporting Information (SI). Also provided in the SI are enthalpies of formation (0 and 298 K), calculated from atomization energies, for species where accurate values may not be available in the prior literature. Additional comparison is made to M06-2X/6-31G(2df,p) relative energies for all minima and transition states (see SI), where the mean absolute deviation between all values is $2.7 \text{ kcal mol}^{-1}$. Comparison is also made to previous G4 level energies, where available, where the mean absolute deviation is $1.0 \text{ kcal mol}^{-1}$.¹⁹

Reaction rate modeling was performed with the MultiWell-2012.1 set of codes.^{23–26} Microscopic rate coefficients are from RRKM theory, based on sums and densities of states for M06-2X structures and G3X-K barrier heights. The energy grained master equation was solved stochastically, from 10^7 independent trajectories of up to 2000 collisions each. An energy grain of 10 cm^{-1} was used, across 2000 grains, with the continuum component of the hybrid master equation formulation evaluated up to $200\,000 \text{ cm}^{-1}$. Quantum mechanical tunnelling is incorporated for H-shift reactions by way of an unsymmetrical Eckart barrier. The bath gas was N_2 , and collisional energy transfer between CN_2OH_4 isomers and N_2 was described using the single exponential-down model with $\Delta E_d = 150 \text{ cm}^{-1}$. Barrierless recombination of $\text{CH}_3\text{N}^\bullet\text{H}$ and $\bullet\text{NO}$ is treated using a restricted Gorin model,²⁷ as described in detail recently.²⁸ The high-pressure limit rate coefficient was set as $7 \times 10^{-11} \text{ cm}^3 \text{ molecule}^{-1} \text{ s}^{-1}$, consistent with the capture rate for the related $\bullet\text{NH}_2 + \bullet\text{NO}$ association.^{29–31} At 298 K the hindrance parameter η was found to be 0.9478 (*syn*)/ 0.9449 (*anti*), with a 2D external rotor of 235.73 (*syn*)/ 251.89 (*anti*) $\text{amu} \text{ \AA}^2$. Simulations were performed at 1 atm pressure at 298 K and at 600–2000 K. Phenomenological rate coefficients at high

temperatures are obtained via the thermal decay method, as implemented in the PPM code.³²

RESULTS

A theoretical energy diagram for the $\text{CH}_3\text{N}^\bullet\text{H} + \bullet\text{NO}$ reaction is provided in Figure 1. Optimized well (**Wn**) and transition state (**TSn**) structures are depicted in Figure 2. Note that

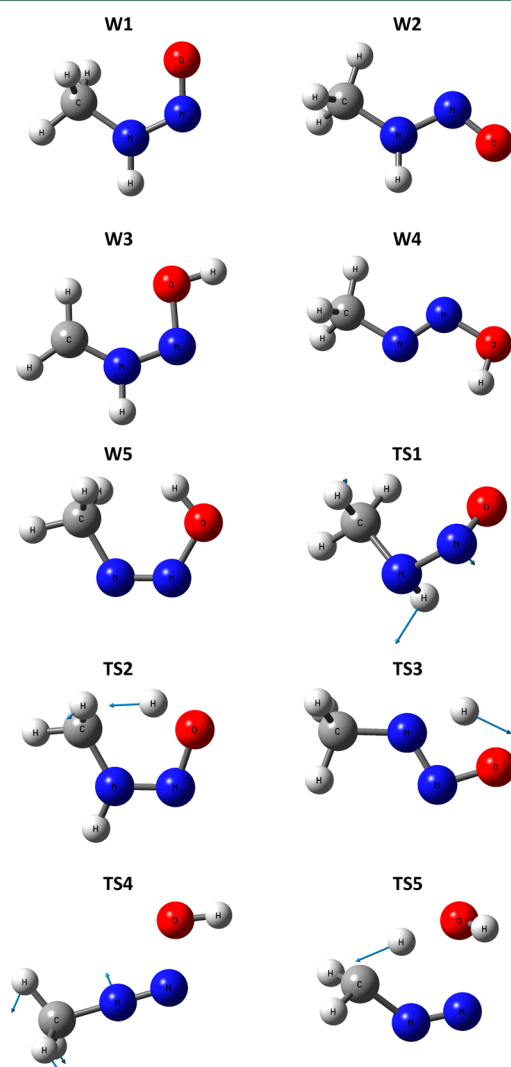


Figure 2. Optimized structures for wells (**Wn**) and transition states (**TSn**) in the $\text{CH}_3\text{N}^\bullet\text{H} + \bullet\text{NO}$ reaction. Calculations at the M06-2X/6-31G(2df,p) level. For transition states, displacement vectors of the imaginary vibrational mode are indicated.

abstraction reactions to form $\text{CH}_2\text{NH} + \text{HNO}$ or HON species require significant barriers,¹⁹ and are not included. We observe from Figure 1 that the $\text{CH}_3\text{N}^\bullet\text{H} + \bullet\text{NO}$ reaction can proceed to form *syn* (**W1**) or *anti* (**W2**) conformations of the CH_3NHNO adduct, with both wells at over 45 kcal mol^{-1} below the reactants. The *syn* conformer is more stable than the *anti* conformer by 1.7 kcal mol^{-1} , placing it at 47.7 kcal mol^{-1} below the reactants. These G3X-K theory energies are in good agreement with G4 theory numbers presented by Tang et al.,¹⁹ which place the respective *syn* and *anti* conformers at 46.7 and 45.4 kcal mol^{-1} below $\text{CH}_3\text{N}^\bullet\text{H} + \bullet\text{NO}$. Interconversion of **W1** and **W2** proceeds via transition state **TS1**, at 25.5 kcal mol^{-1} below the reactants. From **W1**, a 1,4-H shift can take place

(**TS2**) to yield CH_2NHNOH (**W3**), as identified previously.¹⁹ These respective wells and transition states are 7.1 and 20.3 kcal mol^{-1} below the reactant energies, similar to the G4 level reaction energies reported in ref 19 (6.0 and 18.9 kcal mol^{-1} , respectively).

From the *anti*- CH_3NHNO reaction adduct (**W2**) a different pathway is available for isomerization of the primary nitrosamine. The initial step is a 1,3-H shift (**TS3**), producing *trans*- CH_3NNOH (**W4**). This hydrogen shift proceeds at 17.3 kcal mol^{-1} below the energy of the reactants (16.5 kcal mol^{-1} in ref 19), which is lower in energy than the looser 1,4-H shift (**TS2**) due to the more favorable reaction thermodynamics. A *cis*-*trans* isomerization (**TS4**) about the $\text{N}=\text{N}$ double bond then yields **W5**, with barrier 13.3 kcal mol^{-1} below the reactants. We now identify that *cis*- CH_3NNOH (**W5**) can dehydrate via **TS5** to form diazomethane (CH_2NN) and water (denoted as product set **P1**). This dehydration transition state is lower in energy than **TS4** and just above **TS3** at 15.2 kcal mol^{-1} below the reactants. Importantly, dissociation of the chemically activated $[\text{CH}_3\text{NHNO}]^*$ adduct to $\text{CH}_2\text{NN} + \text{H}_2\text{O}$ proceeds via a mechanism with all transition states at least 13 kcal mol^{-1} below the reactant energy. This process is expected to dominate over the formation of **W3** via **TS2**, which is both higher in energy and reversible. Figure 1 also indicates the energy level of the CH_2NN dissociation products ($^1\text{CH}_2 + \text{N}_2 + \text{H}_2\text{O}$), which suggests that if dehydration of the primary nitrosamine does occur, the reaction product might possess sufficient energy to further fragment to singlet methylene and N_2 , depending upon how vibrational energy is portioned among the reaction products.

Master equation kinetic modeling has been performed at 1 atm pressure and 298 K for the chemically activated $\text{CH}_3\text{N}^\bullet\text{H} + \bullet\text{NO}$ reaction based upon the mechanism depicted in Figure 1. Phenomenological rate coefficients at 298 K and 1 atm are listed in Table 1, for use in tropospheric kinetic modeling.

Table 1. Phenomenological Rate Coefficients k for the $\text{CH}_3\text{N}^\bullet\text{H} + \bullet\text{NO}$ Reaction at 298 K and 1 atm N_2^a

reaction	k ($\text{cm}^3 \text{ molecule}^{-1} \text{ s}^{-1}$)
$\text{CH}_3\text{N}^\bullet\text{H} + \bullet\text{NO} \rightarrow \text{CH}_3\text{NHNO}$	7.3×10^{-11}
$\text{CH}_3\text{N}^\bullet\text{H} + \bullet\text{NO} \rightarrow \text{CH}_3\text{NNOH}$	2.0×10^{-11}
$\text{CH}_3\text{N}^\bullet\text{H} + \bullet\text{NO} \rightarrow \text{CH}_2\text{NN} + \text{H}_2\text{O}^b$	3.0×10^{-11}

^aStereoisomers of CH_3NHNO (**W1** + **W2**) and CH_3NNOH (**W4** + **W5**) are summed. Formation of CH_2NHNOH is negligible ($k < 1 \times 10^{-14} \text{ cm}^3 \text{ molecule}^{-1} \text{ s}^{-1}$). ^bAt combustion temperatures (600–2000 K) this rate coefficient can be described using $k = 1.35 \times 10^5 T^{-5.13} \exp(-3760/RT) \text{ cm}^3 \text{ molecule}^{-1} \text{ s}^{-1}$, with T in K and $R = 1.985 \text{ cal mol}^{-1} \text{ K}^{-1}$.

Addition of $\bullet\text{NO}$ to initially form both *syn* (**W1**) and *anti* (**W2**) conformers is considered via separate model runs, with reported rate coefficients representing overall totals. The temporal evolution of wells and products in both the *syn* and *anti* addition processes at 298 K and 1 atm is depicted in Figure 3. Here we observe that in the first few collisions the hot $[\text{CH}_3\text{NHNO}]^*$ adduct predominantly relaxes to populate the wells CH_3NHNO (**W1**, **W2**) and CH_3NNOH (**W4**), along with some ($\sim 10\%$) reverse dissociation to the reactants (designated as **P0**). The vibrationally excited adduct is rapidly deactivated to below the threshold for reverse reaction, but continues to slowly dissociate to $\text{CH}_2\text{NN} + \text{H}_2\text{O}$ (**P1**), with this channel finally accounting for around 20% of the products.

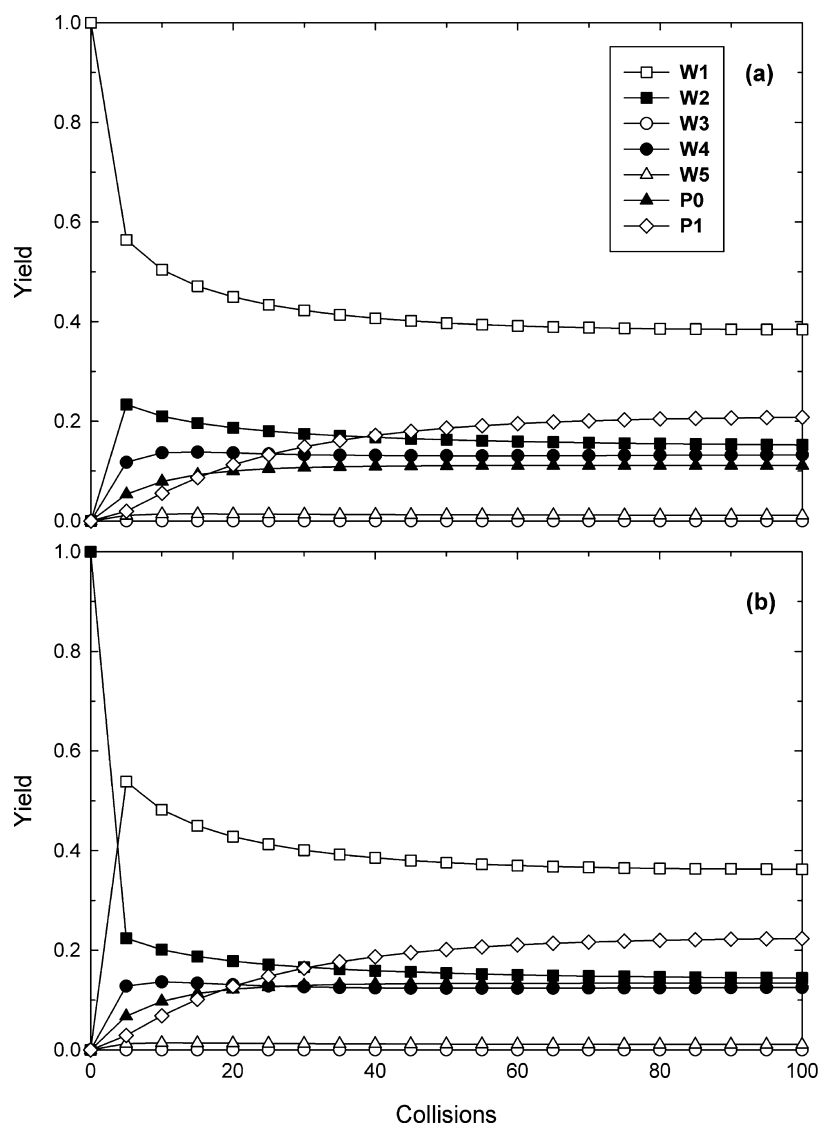


Figure 3. Yields of wells and dissociated product sets as a function of time (collisions) in the chemically activated $\text{CH}_3\text{N}^\bullet\text{H} + \bullet\text{NO}$ reaction via initial recombination to form the (a) *syn* (W1) and (b) *anti* (W2) isomers of CH_3NHNO . Simulations performed at 298 K for 1 atm N_2 .

Once the chemically activated reaction system reaches steady state the main reaction product is *syn*- CH_3NHNO (W1, ~40%), with smaller yields of stabilized *anti*- CH_3NHNO (W2) and *trans*- CH_3NNOH (>10% each). Formation of the CH_2NHNOH isomer W3 as either a stable or transient species is found to be insignificant, at less than 0.01% in both systems. This contradicts the prior work of Tang et al. who assumed that CH_2NHNOH would be a significant product of the $\text{CH}_3\text{N}^\bullet\text{H} + \bullet\text{NO}$ reaction. It thus appears that $\text{R}=\text{NHNOH}$ species will not form in the photochemical oxidation of primary amines.

Branching between chemically activated dissociation to $\text{CH}_2\text{NN} + \text{H}_2\text{O}$ and collisional deactivation of the nitrosamine and diazohydroxide intermediates at ambient temperatures will be sensitive to the selection of ΔE_d , the average energy transferred in deactivating collisions, which is admittedly a relatively poorly known parameter. As such, rate coefficients in the $\text{CH}_3\text{N}^\bullet\text{H} + \bullet\text{NO}$ reaction have been determined as a function of ΔE_d from 50 to 250 cm^{-1} , with the results shown in Figure 4. As expected, with less efficient collisional energy transfer (i.e., smaller ΔE_d values), increased formation of $\text{CH}_2\text{NN} + \text{H}_2\text{O}$ is observed (this is coupled with a somewhat

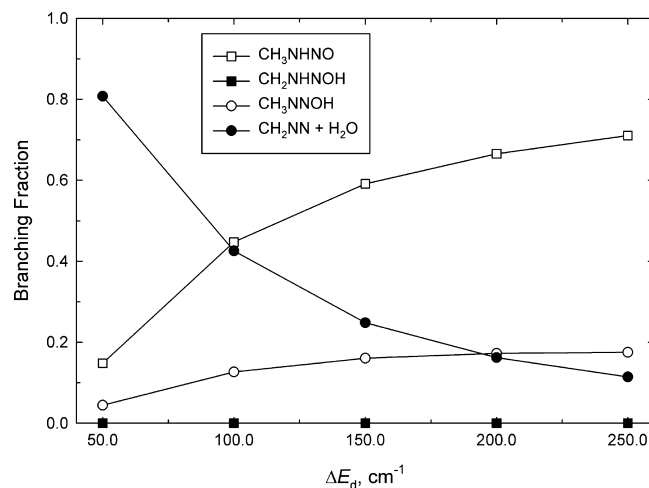


Figure 4. Branching fractions for new product formation in the $\text{CH}_3\text{N}^\bullet\text{H} + \bullet\text{NO}$ reaction as a function of ΔE_d from master equation simulations at 298 K and 1 atm N_2 . Stereoisomers of CH_3NHNO and CH_3NNOH are summed.

slower overall rate of reaction due to an increase in the reverse dissociation process). Slower collisional deactivation also results in an increased ratio of CH_3NNOH to CH_3NHNO , with increased flux over TS3. As ΔE_d is increased, the activated adducts are increasingly trapped as the initial nitrosamine. It is important to note here that across a reasonable range of ΔE_d values the only significant reaction products remain CH_3NHNO , CH_3NNOH , and $\text{CH}_2\text{NN} + \text{H}_2\text{O}$.

The $\text{CH}_3\text{N}^\bullet\text{H} + \bullet\text{NO}$ reaction will also take place in flames, where the nitrogen may originate in the fuel or be incorporated from air (N_2). It is thus useful to apply the reaction model here at combustion temperatures. Master equation modeling has therefore been performed at 600–2000 K and 1 atm N_2 . Rate coefficients at these conditions are plotted in Figure 5. These

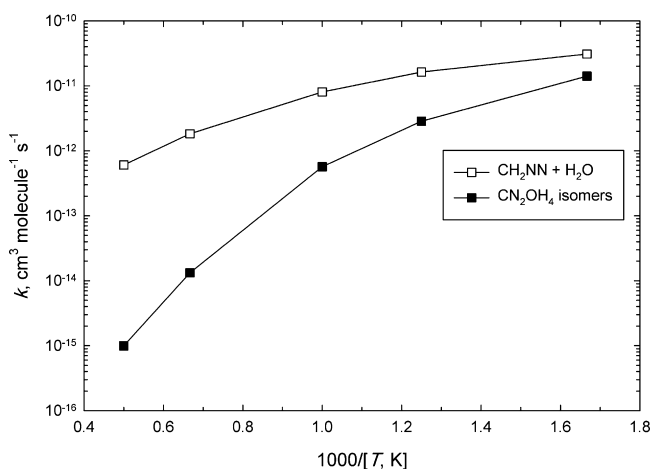


Figure 5. Phenomenological rate coefficients k in the chemically activated $\text{CH}_3\text{N}^\bullet\text{H} + \bullet\text{NO}$ reaction at 1 atm N_2 and 600–2000 K.

results demonstrate that as temperature increases the overall reaction rate decreases, due to a growing importance of the reverse dissociation process. This “negative activation energy” is consistent with results for the related $\bullet\text{NH}_2 + \bullet\text{NO}$ reaction (see ref 31 and references therein). As temperature is increased we also observe increased branching to the $\text{CH}_2\text{NN} + \text{H}_2\text{O}$ product set (P1), and under any real combustion conditions this is expected to be the only major reaction channel. For combustion modeling, this process can be described using the reaction $\text{CH}_3\text{N}^\bullet\text{H} + \bullet\text{NO} \rightarrow \text{CH}_2\text{NN} + \text{H}_2\text{O}$, with $k = 1.35 \times 10^5 T^{-5.13} \exp(-3760/RT) \text{ cm}^3 \text{ molecule}^{-1} \text{ s}^{-1}$ (with T in K and $R = 1.985 \text{ cal mol}^{-1} \text{ K}^{-1}$). Moreover, because CH_2NN will be formed with some degree of excess vibrational energy, and considering that it rapidly decomposes to $^1\text{CH}_2 + \text{N}_2$ at relatively mild temperatures,³³ it is likely that the reaction can simply be treated as $\text{CH}_3\text{N}^\bullet\text{H} + \bullet\text{NO} \rightarrow ^1\text{CH}_2 + \text{N}_2 + \text{H}_2\text{O}$.

DISCUSSION

This work revises our understanding of the products formed from $\bullet\text{NO}$ radical recombination with primary alkylamidogen radicals in the troposphere. Master equation simulations indicate that collisional deactivation of the primary nitrosamine CH_3NHNO will be an important process in this reaction. In the atmosphere the photolysis of CH_3NHNO is expected to be rapid, although it may be able to partition itself into aqueous particles, to some extent. Here, the primary nitrosamine is likely to decompose to N_2 . For secondary nitrosamines such as NDMA, where this decomposition pathway is unavailable, the

gas-phase formation of the stabilized nitrosamine followed by aqueous uptake may provide a source for these carcinogenic compounds in cloud and fog droplets. The ultimate concentration of nitrosamines in these particles would then largely be determined by the magnitude of this source and the rate of photolysis. Our finding that primary nitrosamine formation does occur contradicts a previous computational investigation which suggested that $\text{CH}_2\text{NH} + \text{HO}_2^\bullet + \bullet\text{NO}$ would be the major reaction products, arising from isomerization to CH_2NHNOH followed by reaction with O_2 . Kinetic modeling, however, identifies that CH_2NHNOH will not be formed to any meaningful extent.

Here we have also identified the stabilized alkyl diazohydroxide CH_3NNOH as a product of the $\text{CH}_3\text{N}^\bullet\text{H} + \bullet\text{NO}$ reaction. Importantly, the mechanism for formation of this compound could be extended to alkylamidogen radicals formed from other primary amines, but not secondary amines. The alkyl diazohydroxides are potent alkylating agents, and are implicated as active intermediates in the mechanism of *N*-nitrosamine carcinogenesis.³⁴ Calculations also suggest that CH_3NNOH will not be photolyzed to any significant extent in the troposphere.¹⁹ The possible occurrence and fate of CH_3NNOH and other alkyl diazohydroxides in the atmosphere may therefore need to be considered in the future.

The final product identified in the methylamidogen radical reaction with $\bullet\text{NO}$ is diazomethane, CH_2NN . Again, the mechanism for formation of this compound can be extended to other primary (but not secondary) alkylamidogen radicals. Diazomethane is a highly toxic gas and an efficient alkylating agent. Diazomethane has been previously identified as a product of methylhydrazine ozonolysis in atmospheric chamber studies,³⁵ although its occurrence and chemistry in the atmosphere has not been widely considered. The mechanism developed for the $\text{CH}_3\text{N}^\bullet\text{H} + \bullet\text{NO}$ reaction indicates that the $\text{CH}_2\text{NN} + \text{H}_2\text{O}$ product set will be produced with between about 45 and 60 kcal mol^{-1} excess vibrational energy. In comparison, the barrier for CH_2NN dissociation is about 37 kcal mol^{-1} (and the experimental activation energy is 34 kcal mol^{-1}).³³ The vibrational energy in the product fragments will be partitioned between CH_2NN (9 internal degrees of freedom) and H_2O (3 internal degrees of freedom), and it is foreseeable that some fraction of the CH_2NN population will have sufficient vibrational energy to promptly dissociate to $^1\text{CH}_2$ and N_2 . In the troposphere, singlet methylene may recombine with N_2 , or be collisionally quenched down to the triplet ground-state.³⁶ Following intersystem crossing, association of $^3\text{CH}_2$ with O_2 can take place,³⁶ leading to the Criegee intermediate (carbonyl oxide) CH_2OO .

To further advance our understanding of the importance of primary nitrosamines, alkyl diazohydroxides, and diazoalkanes in the atmosphere, field and laboratory observations are required. Based on the present work, though, we can begin to constrain the formation rates of some of these compounds. In an urban air mass near a significant methylamine source we might expect methylamine mixing ratios of around 1 ppb,² with daytime OH concentrations of ca. $10^7 \text{ molecules cm}^{-3}$. Assuming that the $\text{CH}_3\text{NH}_2 + \bullet\text{OH}$ reaction proceeds at $1.7 \times 10^{-11} \text{ cm}^3 \text{ molecule}^{-1} \text{ s}^{-1}$,⁷ and that $\text{CH}_3\text{N}^\bullet\text{H}$ accounts for 20% of the reaction products,⁸ we estimate a $\text{CH}_3\text{N}^\bullet\text{H}$ radical production rate of about 100 ppt/hour. This radical will react slowly with O_2 , and reactions with $\bullet\text{NO}$ and NO_2^\bullet should be the dominant atmospheric sinks. Even at relatively low total NO_x levels of ~ 1 ppb the lifetime of $\text{CH}_3\text{N}^\bullet\text{H}$ toward $\bullet\text{NO}$ and NO_2^\bullet will be

short (<1 s), with $\text{CH}_3\text{N}^\bullet\text{H}$ quantitatively converted into new products under even relatively pristine conditions. Assuming a $\bullet\text{NO}:\text{NO}_2^\bullet$ ratio of 1:1, and using branching fractions determined here, we then estimate representative daytime tropospheric formation rates on the order of 10 ppt/hour for the alkyldiazohydroxide CH_3NNOH and the diazoalkane CH_2NN and around 30 ppt/hour for the primary nitrosamine CH_3NHNO . Note that these formation rates will be most sensitive to the actual level of methylamine present as well as the partitioning of NO_x between NO^\bullet and $\bullet\text{NO}_2$, which could both vary substantially.

To begin to estimate atmospheric levels of CH_3NNOH , CH_2NN , and CH_3NHNO we need to understand their atmospheric lifetimes. Photolysis will predominantly control the lifetimes of CH_3NHNO and CH_2NN and thus the levels to which they can accumulate. Photolysis is not, however, thought to be a major sink for CH_3NNOH , which is likely to instead react with $\bullet\text{OH}$ or partition into the particle phase. The $\text{CH}_3\text{NNOH} + \bullet\text{OH}$ reaction would proceed via H abstraction, but is expected to be relatively fast given that the resultant radical would be stabilized by the resonance forms $\bullet\text{CH}_2-\text{N}=\text{N}-\text{OH}$ and $\text{CH}_2=\text{N}-\text{N}^\bullet-\text{OH}$. If the CH_3NNOH lifetime is assumed to be in the range of 6 to 24 h (typical for short-lived VOCs), then steady-state CH_3NNOH concentrations of tens to hundreds of parts per trillion are achieved. This estimate needs refining, but shows that alkyldiazohydroxides may accumulate to levels that are significant with respect to their parent amine (in this case 1 ppb). To better quantify the importance of CH_3NNOH in the atmosphere further work is needed for verifying branching fractions for the different product sets of the $\text{CH}_3\text{N}^\bullet\text{H} + \bullet\text{NO}$ reaction, as well as an improved understanding of the $\text{CH}_3\text{NNOH} + \text{OH}$ reaction and other atmospheric sinks for this compound.

CONCLUSIONS

This work has identified that primary alkylaminyl free radicals can react with $\bullet\text{NO}$ under tropospheric conditions to yield primary nitrosamines, along with alkyldiazohydroxides and diazoalkanes. These findings refute those of previous studies that have suggested imines ($+\text{HO}_2^\bullet + \text{NO}^\bullet$) are the major reaction products. The $\text{CH}_3\text{N}^\bullet\text{H} + \bullet\text{NO}$ reaction is found to yield CH_3NHNO , CH_3NNOH , and CH_2NN ($+ \text{H}_2\text{O}$) as significant products, all three of which are potentially toxic and may need to be considered as byproducts from the tropospheric oxidation of amines. The alkyldiazohydroxide CH_3NNOH is of particular interest as it is not expected to be lost through photolysis and here is estimated to accumulate to tropospheric levels that are significant relative to those of the parent amine.

ASSOCIATED CONTENT

Supporting Information

Optimized structures, vibrational frequencies, and moments of inertia for CN_2OH_4 stationary points. Calculated enthalpies of formation for selected minima. Energy diagram with M06-2X/6-31G(2df,p) energies. This material is available free of charge via the Internet at <http://pubs.acs.org>.

AUTHOR INFORMATION

Corresponding Author

*E-mail: gdasilva@unimelb.edu.au.

Notes

The authors declare no competing financial interest.

ACKNOWLEDGMENTS

This work was supported by the Australian Research Council through Discovery Project DP110103889.

REFERENCES

- (1) Schade, G. W.; Crutzen, P. J. Emission of aliphatic amines from animal husbandry and their reactions: Potential source of N_2O and HCN . *J. Atmos. Chem.* **1995**, *22*, 319–346.
- (2) Ge, X.; Wexler, A. S.; Clegg, S. L. Atmospheric amines - Part I. A review. *Atmos. Environ.* **2011**, *45*, 524–546.
- (3) Ge, X.; Wexler, A. S.; Clegg, S. L. Atmospheric amines - Part II. Thermodynamic properties and gas/particle partitioning. *Atmos. Environ.* **2011**, *45*, 561–577.
- (4) Roberts, J. M.; et al. Isocyanic acid in the atmosphere and its possible link to smoke-related health effects. *Proc. Natl. Acad. Sci., U. S. A.* **2011**, *108*, 8966–8971.
- (5) Young, P. J.; et al. Isocyanic acid in a global chemistry transport model: Tropospheric distribution, budget, and identification of regions with potential health impacts. *J. Geophys. Res.* **2012**, *117*, D10308.
- (6) Atkinson, R.; Perry, R. A.; Pitts, J. N., Jr. Rate constants for the reaction of the OH radical with $(\text{CH}_3)_2\text{NH}$, CH_3SH and CH_3NH_2 over the temperature range 299–426 K. *J. Chem. Phys.* **1977**, *66*, 1578–1581.
- (7) Carl, S. A.; Crowley, J. N. Sequential two (blue) photon absorption by NO_2 in the presence of H_2 as a source of OH in pulsed photolysis kinetic studies: Rate constants for reaction of OH with CH_3NH_2 , $(\text{CH}_3)_2\text{NH}$, $(\text{CH}_3)_3\text{N}$, and $\text{C}_2\text{H}_5\text{NH}_2$ at 295 K. *J. Phys. Chem. A* **1998**, *102*, 8131–8141.
- (8) Galano, A.; Alvarez-Idaboy, J. R. Branching ratios of aliphatic amines + OH gas-phase reactions: A variational transition-state theory study. *J. Chem. Theory Comput.* **2008**, *4*, 322–327.
- (9) Ly, T.; Kirk, B. B.; Hettiarachchi, P. I.; Poad, B. L. J.; Trevitt, A. J.; da Silva, G.; Blanksby, S. J. Reactions of simple and peptidic α -carboxylate radical anions with dioxygen in the gas phase. *Phys. Chem. Chem. Phys.* **2011**, *13*, 16314–16323.
- (10) da Silva, G.; Kirk, B. B.; Lloyd, C.; Trevitt, A. J.; Blanksby, S. J. Concerted HO_2 elimination from α -aminoalkylperoxyl free radicals: Experimental and theoretical evidence from the gas-phase $\text{NH}_2^\bullet\text{CHCO}_2^- + \text{O}_2$ reaction. *J. Phys. Chem. Lett.* **2012**, *3*, 805–811.
- (11) da Silva, G. Atmospheric chemistry of 2-aminoethanol (MEA): Reaction of the $\text{NH}_2^\bullet\text{CHCH}_2\text{OH}$ radical with O_2 . *J. Phys. Chem. A* **2012**, *116*, 10980–10986.
- (12) Rudic, S.; Murray, C.; Harvey, J. N.; Orr-Ewing, A. J. The product branching and dynamics of the reaction of chlorine atoms with methylamine. *Phys. Chem. Chem. Phys.* **2003**, *5*, 1205–1212.
- (13) Magee, P. N.; Barnes, J. M. The production of malignant primary hepatic tumours in the rat by feeding dimethylnitrosamine. *Br. J. Cancer* **1956**, *10*, 114–122.
- (14) Herckes, P.; Leenheer, J. A.; Collett, J. L. Comprehensive characterization of atmospheric organic matter in Fresno, California fog water. *Environ. Sci. Technol.* **2007**, *41*, 393–399.
- (15) Hutchings, J. W.; Ervens, B.; Straub, D.; Herckes, P. N-Nitrosodimethylamine occurrence, formation and cycling in clouds and fogs. *Environ. Sci. Technol.* **2010**, *44*, 8128.
- (16) da Silva, G.; Dlugogorski, B. Z.; Kennedy, E. M. Elementary reaction step model of the N-nitrosation of ammonia. *Int. J. Chem. Kinet.* **2007**, *39*, 645–656.
- (17) da Silva, G.; Kennedy, E. M.; Dlugogorski, B. Z. Nucleophilic catalysis of nitrosation: Relationship between nitrosating agent equilibrium constant and catalyst nucleophilicity. *J. Chem. Res. (S)* **2002**, 589–590.
- (18) da Silva, G.; Kennedy, E. M.; Dlugogorski, B. Z. Effect of added nucleophilic species on the rate of primary amino acid nitrosation. *J. Am. Chem. Soc.* **2005**, *127*, 3664–3665.

- (19) Tang, Y.; Hanrath, M.; Nielsen, C. J. Do primary nitrosamines form and exist in the gas phase? A computational study of CH_3NHNO and $(\text{CH}_3)_2\text{NNO}$. *Phys. Chem. Chem. Phys.* **2012**, *14*, 16365–16370.
- (20) Tang, Y.; Nielsen, C. J. Theoretical study on the formation and photolysis of nitrosamines ($\text{CH}_3\text{CH}_2\text{NHNO}$ and $(\text{CH}_3\text{CH}_2)_2\text{NNO}$) under atmospheric conditions. *J. Phys. Chem. A* **2013**, *117*, 126–132.
- (21) da Silva, G. G3X-K theory: A composite theoretical method for thermochemical kinetics. *Chem. Phys. Lett.* **2013**, *558*, 109–113.
- (22) Frisch, M. J.; Trucks, G. W.; Schlegel, H. B.; Scuseria, G. E.; Robb, M. A.; Cheeseman, J. R.; Scalmani, G.; Barone, V.; Mennucci, B.; Petersson, G. A.; Nakatsuji, H.; Caricato, M.; Li, X.; Hratchian, H. P.; Izmaylov, A. F.; Bloino, J.; Zheng, G.; Sonnenberg, J. L.; Hada, M.; Ehara, M.; Toyota, K.; Fukuda, R.; Hasegawa, J.; Ishida, M.; Nakajima, T.; Honda, Y.; Kitao, O.; Nakai, H.; Vreven, T.; Montgomery, J. A., Jr.; Peralta, J. E.; Ogliaro, F.; Bearpark, M.; Heyd, J. J.; Brothers, E.; Kudin, K. N.; Staroverov, V. N.; Kobayashi, R.; Normand, J.; Raghavachari, K.; Rendell, A.; Burant, J. C.; Iyengar, S. S.; Tomasi, J.; Cossi, M.; Rega, N.; Millam, J. M.; Klene, M.; Knox, J. E.; Cross, J. B.; Bakken, V.; Adamo, C.; Jaramillo, J.; Gomperts, R.; Stratmann, R. E.; Yazyev, O.; Austin, A. J.; Cammi, R.; Pomelli, C.; Ochterski, J. W.; Martin, R. L.; Morokuma, K.; Zakrzewski, V. G.; Voth, G. A.; Salvador, P.; Dannenberg, J. J.; Dapprich, S.; Daniels, A. D.; Farkas, O.; Foresman, J. B.; Ortiz, J. V.; Cioslowski, J.; Fox, D. J. *Gaussian 09*, revision B.01; Gaussian, Inc.: Wallingford, CT, 2010.
- (23) *MultiWell-2012.1 Software*. Designed and maintained by Barker, J. R., with contributors Ortiz, N. F.; Preses, J. M.; Lohr, L. L.; Maranzana, A.; Stimac, P. J.; Nguyen, T. L.; Kumar, T. J. D.; University of Michigan: Ann Arbor, MI, 2012; <http://aoss.engin.umich.edu/multiwell/>.
- (24) Barker, J. R. Multiple-well, multiple-path unimolecular reaction systems. I. MultiWell computer program suite. *Int. J. Chem. Kinet.* **2001**, *33*, 232–245.
- (25) Barker, J. R. Energy transfer in master equation simulations: A new approach. *Int. J. Chem. Kinet.* **2009**, *41*, 748–763.
- (26) Nguyen, T. L.; Barker, J. R. Sums and densities of fully coupled anharmonic vibrational states: A comparison of three practical methods. *J. Phys. Chem. A* **2010**, *114*, 3718–3730.
- (27) Smith, G. P.; Golden, D. M. Application of RRKM theory to the reactions of $\text{OH} + \text{NO}_2 + \text{N}_2 \rightarrow \text{HONO}_2 + \text{N}_2$ (1) and $\text{ClO} + \text{NO}_2 + \text{N}_2 \rightarrow \text{ClONO}_2 + \text{N}_2$ (2); a modified Gorin model transition state. *Int. J. Chem. Kinet.* **1978**, *10*, 489–501.
- (28) da Silva, G. Reaction of methacrolein with the hydroxyl radical in air: Incorporation of secondary O_2 addition into the $\text{MACR} + \text{OH}$ master equation. *J. Phys. Chem. A* **2012**, *116*, 5317–5324.
- (29) Phillips, L. F. A *priori* rate constant for the reaction $\text{NH}_2 + \text{NO} \rightarrow \text{N}_2 + \text{H}_2\text{O}$. *Chem. Phys. Lett.* **1987**, *135*, 269–274.
- (30) Diau, E. W.-G.; Smith, S. C. Temperature dependence of rate coefficients and branching ratios for the $\text{NH}_2 + \text{NO}$ reaction via microcanonical variational transition state theory. *J. Phys. Chem.* **1996**, *100*, 12349–12354.
- (31) Miller, J. A.; Klippenstein, S. J. Theoretical considerations in the $\text{NH}_2 + \text{NO}$ reaction. *J. Phys. Chem. A* **2000**, *104*, 2061–2069.
- (32) Pinches, S. J.; da Silva, G. On the separation of timescales in chemically activated reactions. *Int. J. Chem. Kinet.* **2013**, *45*, 387–396.
- (33) Setser, D. W.; Rabinovitch, B. S. Singlet methylene from thermal decomposition of diazomethane. Unimolecular reactions of chemically activated cyclopropane and dimethylcyclopropane molecules. *Can. J. Chem.* **1962**, *40*, 1425–1451.
- (34) Lijinsky, W. Nucleic acid alkylation by *N*-nitroso compounds related to organ-specific carcinogenesis. In *Chemical Carcinogens*; Politzer, P., Martin, F. J., Jr., Eds.; Elsevier: Amsterdam, 1988; pp 242.
- (35) Tuazon, E. C.; Carter, W. P.; Winer, A. M.; Pitts, J. N., Jr. Reactions of hydrazines with ozone under simulated atmospheric conditions. *Environ. Sci. Technol.* **1981**, *15*, 823–828.
- (36) Laufer, A. H. Kinetics of gas phase reactions of methylene. *Rev. Chem. Intermediates* **1981**, *4*, 225–257.